Analysis of island morphology in a model for Pb-mediated growth of Ge on Si(111)

Janusz Bęben,[1,2,*] Ing-Shouh Hwang,[1] and Tien T. Tsong[1]
[1]*Institute of Physics, Academia Sinica, Nankang, Taipei, Taiwan, Republic of China*
[2]*Institute of Experimental Physics, Wrocław University, Wrocław, Poland*
(Received 28 May 2001; revised manuscript received 9 July 2001; published 28 November 2001)

Analysis of island morphology in a realistic model of surfactant-mediated epitaxial growth is presented and compared with experimental results obtained for Pb-mediated growth of Ge on Si(111). In kinetic Monte Carlo simulations it is found that the clustering of Ge atoms above the surfactant obeys an anomalous scaling, and that the cluster size distribution is self-similar in time, up to the latest stages of coarsening, where Ostwald ripening predominates. The clustering process is limited in time due to the irreversible exchange of Ge atoms with surfactant. Further growth of islands below surfactant leads to their ramification. Islands which do not significantly grow below surfactant are compact, and are characterized by a size distribution whose shape is similar to that obtained within the cluster diffusion model of crystal growth.

DOI: 10.1103/PhysRevB.64.235328 PACS number(s): 68.55.−a, 61.43.Hv, 02.70.Uu

I. INTRODUCTION

The active materials which suppress a formation of three-dimensional islands during epitaxial growth of thin films are called surfactants.[1,2] They modify the growth of epitaxial layers on metal[3,4] or semiconductor substrates,[5–11] as well as on insulator surfaces.[12,13] In the presence of a surfactant, a layer-by-layer growth can be achieved; this is of great importance for fabricating advanced electronic devices. Usually a monolayer of surfactant is initially deposited onto the substrate, and when the growth proceeds, the surfactant segregates to the surface.

The surfactant-mediated epitaxy (SME) of semiconductors has been extensively studied, especially on silicon substrates. It has been shown that different surfactants may modify the epitaxial growth in quite a different way,[14] but the underlying growth mechanism is still poorly understood. Hibino *et al.*[15] reported a study of growth of Ge islands on a Si(111)-$\sqrt{3}\times\sqrt{3}$ surface with 1/3 monolayer of deposited Pb atoms. One monolayer Pb surfactant promoted layer by layer growth of Ge on Si(111) has been studied recently by Hwang *et al.*[16,18] and Chang *et al.*[17] They examined the initial stages (submonolayer coverages) of Ge on Si(111) with Pb as the surfactant using the scanning tunneling microscope (STM) technique. They found characteristic features considerably different from those observed in non-SME growth: (i) The existence of a pronounced, and almost temperature-independent threshold coverage below which no islands grow. (ii) The transition in the island shape (compact to fractallike) caused by raising temperature or lowering the coverage or deposition flux. (iii) Coverage dependence of island density opposite to non-SME systems.

A few models were proposed to explain the surfactant-mediated growth,[5,19–29] but none explains all the essential features of the Ge/Pb/Si(111) films. These features are interrelated: For example, a mechanism proposed to explain the temperature-dependence of the island shape has also to yield an almost temperature-independent threshold coverage for nucleation. In our previous paper[30] we proposed a model of SME which does have this property. Experimental study of the time evolution is rather difficult. No such data have apparently been obtained as yet, and at present the time evolution is best probed in simulations. Here we extend our previous study[30] to the analysis of the time evolution of island size distributions and their scaling properties.

II. MODEL SUMMARY

The kinetic Monte Carlo method[31,32] used in our previous[30] and present studies makes the assumption of Markovian dynamics throughout. The assumption holds because of the high values of the ratio $\Delta E/kT$ we use in our simulations. For a jump of a monomer at 400 K the ratio is about 19. Because we use a Hamiltonian which fixes the static properties of the steady state, the dynamics is not revealed.

In our model of surfactant-mediated growth the substrate is covered by a surfactant monolayer. The growing material is deposited at a constant rate onto the surfactant, and can then diffuse and reversibly nucleate. The interaction between nearest-neighbor atoms is taken into account by bond counting, and it is assumed that atoms in dimers repel each other. This assumption of our model is based on experimental results by Tsong and Casanova.[33] Atoms above the surfactant can exchange position with surfactant and stick irreversibly to the substrate. We use the expression ''clusters'' for aggregates of atoms above the surfactant. The ''islands'' refer to aggregates after exchange. A cluster size-dependent barrier for exchange is assumed. Islands can grow further in account of incoming monomers and clusters. For details see Ref. 30.

Under these assumptions our model explains the experimentally observed[16–18] existence of a threshold coverage. It also explains the transition in island shape due to coverage, temperature, and deposition flux, as well as the temperature dependence of island density. Additionally, we show in Fig. 1(a) transition in island shape due to deposition flux which was not presented in our previous paper.[30] Experimental results are qualitatively similar, though the increase of island density is faster [see Fig. 3(b) of Ref. 16]. The shape of islands at low- and high-flux rates are shown in the insets.

III. ISLAND SIZE DISTRIBUTION

The evolution of submonolayer island morphology during epitaxial growth leads to a final island size distribution which

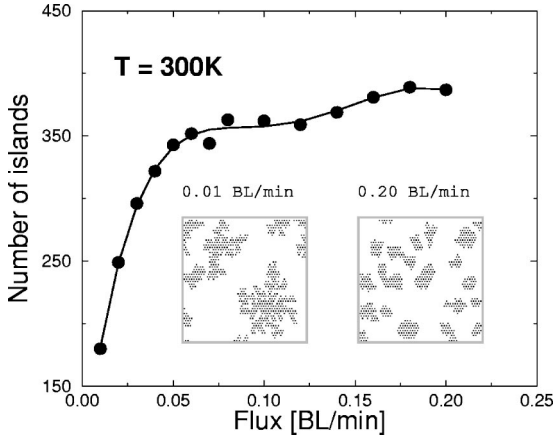

FIG. 1. Simulation of the flux dependence of island density. Insets are snapshots of island morphology. $\theta = 0.3$ ML. The simulation area consists of 67 500 adsorption sites.

reflects the growth mechanism.[34,35] Epitaxial layers grow during deposition, and when the system is not quenched the growth continues even after the deposition. Simulation results have shown that changes in island morphology which take place after the deposition are crucial.

Figures 2 and 3 show changes in the cluster and the island size distributions during growth of the fractal (at $\theta = 0.10$) and of the compact (at $\theta = 0.25$) islands, respectively. Temperature is 300 K, and the deposition flux is 0.2 BL/min.

Figures 2(a) and 3(a) show the cluster size distributions at a time when the deposition is completed. The number of monomers is written into the diagrams if their values are out of the vertical-axis range. A monotonous decay with size is observed, and no islands are formed so far. The growth occurs after deposition, and looks different for the two growth modes. The fractallike growth (Fig. 2) is characterized by a low island density and by an island growth which is actuated by the incoming monomers. At 700 s of elapsed time the monomers dominate, and contribute to the growth of the already formed islands. The process of island formation is

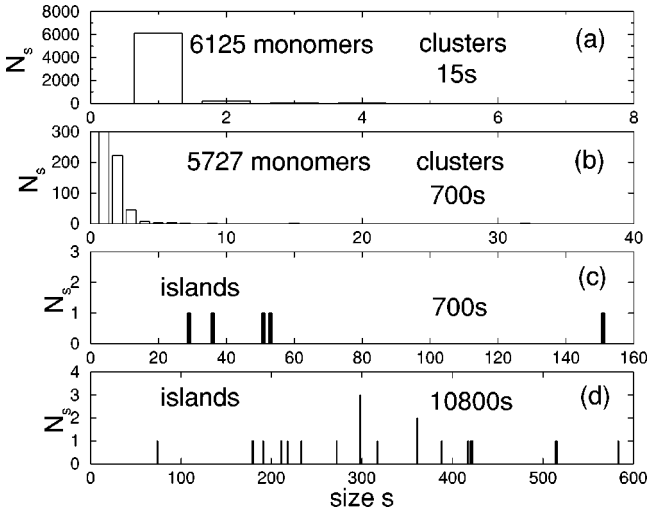

FIG. 2. Time evolution of the cluster and island size distributions at $\theta = 0.10$ ML.

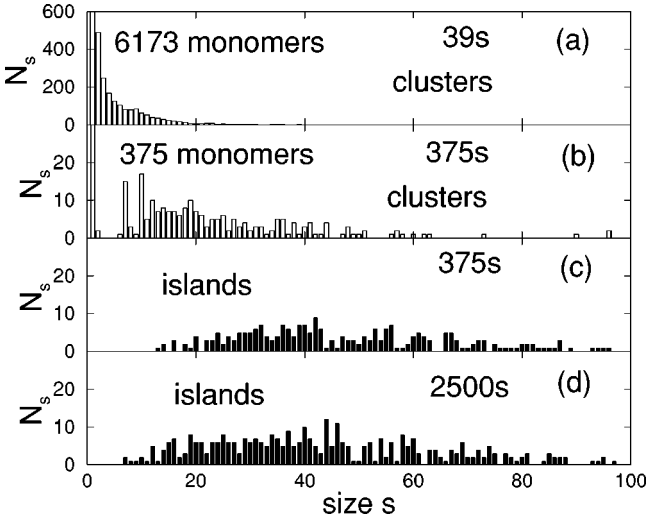

FIG. 3. Time evolution of the cluster and island size distributions at $\theta = 0.25$ ML.

slow. It takes about 10 800 s until the final distribution is formed [Fig. 2(d)]. Note that horizontal-axis scales for Figs. 2(a)–2(d) are different.

The growth of compact islands is presented in Fig. 3. They are formed much faster than fractal ones, and it takes about 2500 s to reach the final distribution [Fig. 3(d)]. Already after 375 s, however, the number of monomers is considerably reduced, and there is a large number of small clusters and islands. A characteristic gap between the stable compact clusters and the monomers is formed [Fig. 3(b)], and two distinct peaks appear in the cluster distribution. They correspond to stable clusters consisting of 7 and 10 atoms, respectively (see Fig. 4).

The final distribution at 2500 s does not differ much from that at $t = 375$ s because the clusters formed above surfactant do not significantly grow after exchange with the surfactant. Note also that there is a common horizontal-axis scale for Figs. 4(a)–4(d).

The data presented in Figs. 2 and 3 are obtained during one simulation run for illustrating the growth mechanism only. The poor statistic seen in Fig. 2 is due to the small number of large fractallike islands which grow close to the threshold coverage. Quantitative analysis of large fractal islands is not a subject of this paper. It can be done for example by calculating the fractal dimension of a single aggregate and by analyzing its dependence on simulation parameters. This will be a subject of our future study.

Figure 5 shows the time evolution of the average size s_{av}, and of the total number N of the clusters and of the islands. During the deposition time no islands grow, and there is a powerlike increase of the number of clusters in time [Figs. 5(a) and 5(c)]. The changes after the deposition differ de-

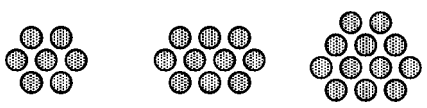

FIG. 4. Stable clusters containing 7, 10, and 12 atoms. All atoms have at least three bonds with nearest neighbors.

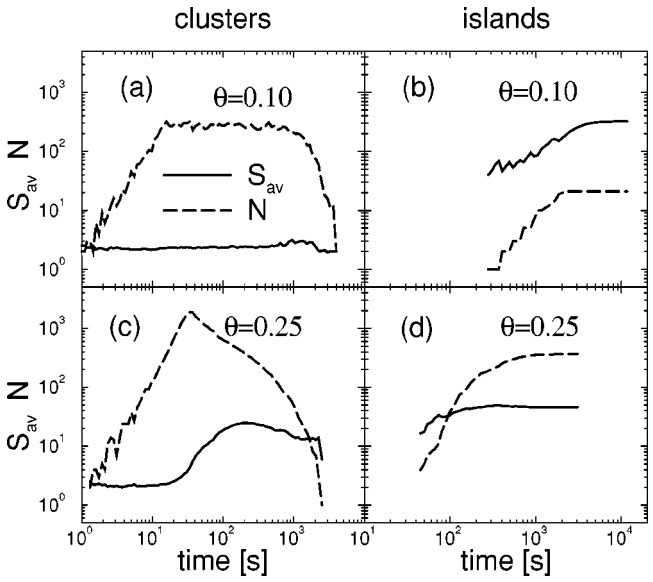

FIG. 5. Time evolution of clusters and islands. The solid lines are the average sizes s_{av} while the dashed lines are the total number N of clusters or islands.

pending on the growth mode. The average island size is a basic value in the ''universal'' scaling approach of the island size distribution,[36,37] and is discussed in detail in the next section.

A. Scaling

The island size distribution has been examined for homoepitaxial[38–40] as well as for heteroepitaxial[41] systems, and a quantitative scaling analysis has been done for homoepitaxy of Fe(100) (Ref. 40) and for heteroepitaxy of Cu on Ni(100).[42] The results confirm the ''universal'' scaling formula[36,37]

$$N_s \sim \theta s_{av}^{-2} f(s/s_{av}), \tag{1}$$

where N_s is the island density of size s, f is the scaling function, $\theta = \Sigma_{s \geqslant 1} s N_s$ is the coverage, and $s_{av} = \theta / \Sigma_{s \geqslant 1} N_s$.

This scaling was found to describe growth of islands under a constant deposition flux. The post deposition growth and its scaling properties have been studied by Li *et al.*[43] who assumed the ''universal'' scaling formula (1) with $s_{av} \sim \theta^{-z}$, so that

$$N_s(\theta) \sim \theta^{2z+1} f(s\theta^z), \tag{2}$$

where z is a constant and f is a scaling function which satisfies the relation

$$\int_0^\infty f(u)du = \int_0^\infty u f(u)du. \tag{3}$$

The total island density therefore scales as $N \sim \theta^{z+1}$. If the constant $z \neq 0$ then the scaling is anomalous, and z is related to the critical cluster size. The anomalous scaling has been found for the point island model, large critical sizes, and for low coverages.[43]

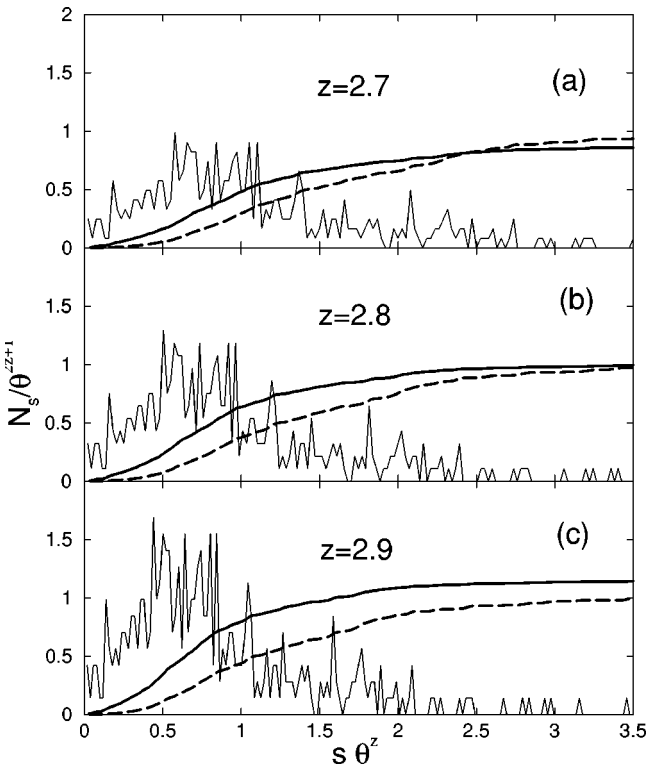

FIG. 6. The island size distribution in simulated data scaled with different exponents z. $T = 300$ K and $\theta = 0.26$ ML. Solid and dashed lines are cumulative sums of the left- and right-hand side integrals of Eq. (3), respectively.

In our model of SME a post nucleation growth dominates, and we therefore apply the scaling by Li *et al.*[43] to our simulated and experimental results. We find the exponent z by comparison of the left- and right-hand side integrals of Eq. (3).

Figure 6 illustrates the procedure. The simulated island size distributions have been scaled according to Eq. (2), with parameters $z = 2.7$, 2.8, and 2.9. Figure 6(b) shows the case where both integrals are equal (the cumulative sums meet). For lower and higher values of z the integrals differ. An example of applying the above procedure is presented in Fig. 7. The scaled curves [Fig. 7(b)] overlap after applying the scaling procedure.

The exponents z turn out to be coverage dependent, with a minimum at about 0.16 ML [Fig. 8(a)]. The origin of the minimum is not clear, but it may be related to the transition in island shape in the coverage range considered. For the two dimensional point island model[43] it has been shown that if $z = 0$, 0.24, and 0.65 then the critical cluster sizes are 1, 2, and 3, respectively. Our model is more realistic, and does not assume a constant critical cluster size during simulation run. This will be discussed in Sec. IV. Nevertheless, the z values larger than 2 show that the scaling is anomalous and that the critical clusters are large.

As mentioned above, the anomalous scaling introduces a scaling exponent z which can be determined from the single island size distribution. The exponents z found this way can then serve to reproduce the coverage dependence of the average island size, s_{av}, and the total island density, N [Figs.

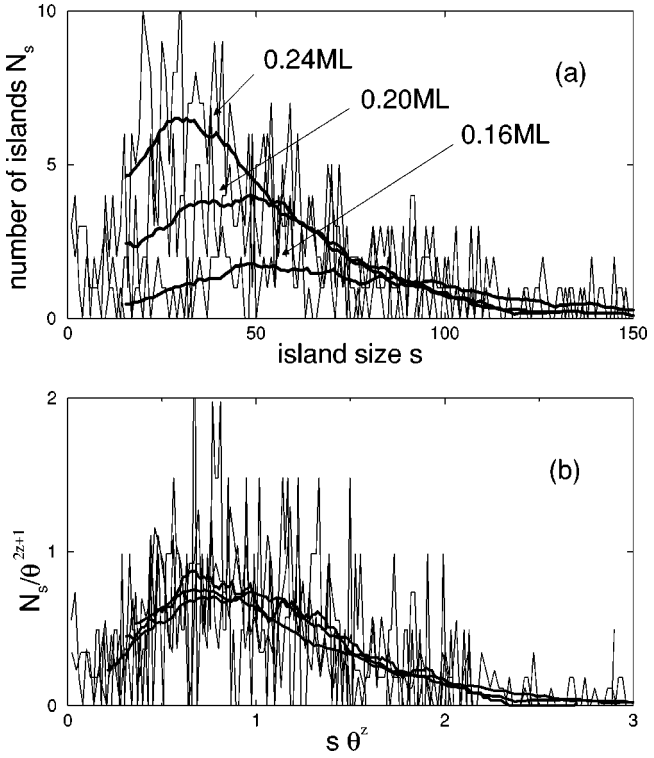

FIG. 7. Scaled (a) and unscaled (b) island size distributions. Thick lines are averages over 30 points taken for better viewing. The parameters z are 2.64, 2.43, and 2.33 at $\theta = 0.24$, 0.20, and 0.16 ML, respectively.

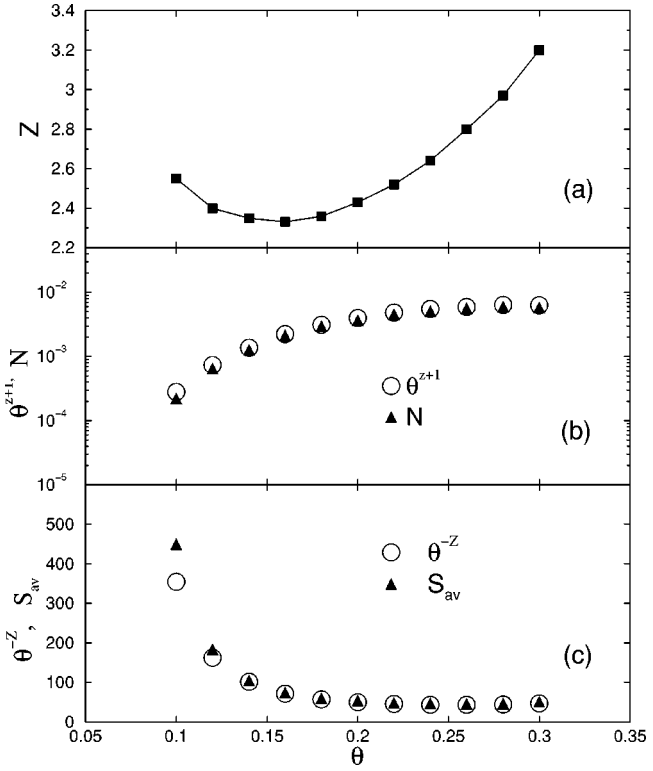

FIG. 8. (a) Coverage dependence of the parameter z, (b) total island density N, and (c) average cluster size s_{av}. Open circles are values calculated from the exponent z. Full triangles are data obtained from simulations.

8(b) and 8(c)]. The points merge nicely except at low coverages where the island density is low and therefore statistic poor. This procedure is equivalent to the overlapping of the scaled island size distributions, as presented in Fig. 7(b). The advantage is that the comparison is more clear.

A similar procedure of finding the exponent z is applied to the experimental data after evaluating the size of the STM images. The resolution of experimental images is about 4000 Å/256 pixels. Assuming the distance between Ge atoms in the island to be 3.6 Å we conclude that one pixel of the STM image corresponds to about 19 atoms. Figure 9 shows the results. Note that the maxima of the scaled curves correspond to normalized sizes smaller than 1 for both the simulated [Fig. 7(b)] and for the experimental [Fig. 9(b)] results. These will be discussed in the next section.

B. Shape of the scaling functions

In our model of SME the growth process consists of deposition, aggregation, and cluster growth, followed by growth of islands. The crucial part is the second one. An atom can join a cluster, dissociate from it, or move along its edges. As a result, the cluster mass center undergoes a random walk equivalent to mass transport. The cluster diffusion model seems to be appropriate in describing the shape of the scaling function. The model originates from the mean-field approximation due to Smoluchowski and co-workers[26,44–47] and assumes a size-, s, dependent diffusion coefficient $D(s) \sim s^{-\xi}$. The exponent ξ is related to the macroscopic mechanism responsible for the cluster displacement.

The shape of the scaling functions in the cluster diffusion model has been examined by Kandel.[26] He found that there exists a one-parameter family of scaling functions which obeys the rate equation. Simulations show[26] that one function out of the family is physically reasonable. It has a maximum at about 0.5 (see Fig. 3 of Ref. 26). Our simulated and experimental island size distributions reveal a similar shape, characterized by maxima at normalized sizes smaller than 1 [see Figs. 7(b) and 9(b)]. Similar shapes of island size distribution have been found in octadecylphosphonic acid deposited on mica from a solution,[48] and also in simulation results based on the Clarke-Vvedensky model of thin-film growth.[49] The common assumptions of ours and the Clarke-Vvedensky models is the reversible cluster growth and calculation of the nearest-neighbors interactions by bond counting. We conclude therefore that cluster diffusion is an important element of island formation in our model of SME.

Island size distribution has been studied also for non-SME growth of Fe/Fe(001) (Ref. 40) and Cu/Ni(000).[42] In both systems the critical cluster sizes were found to be small (1 or 2), and the island size distributions were characterized by maxima at normalized sizes close to 1.

IV. LIMIT OF CLUSTER GROWTH WITH NO EXCHANGE

In our model the growth of clusters above the surfactant is limited by the exchange mechanism with surfactant atoms. The exchange is irreversible, and buried atoms cannot move. This leads to a final island morphology in a limited time. It is

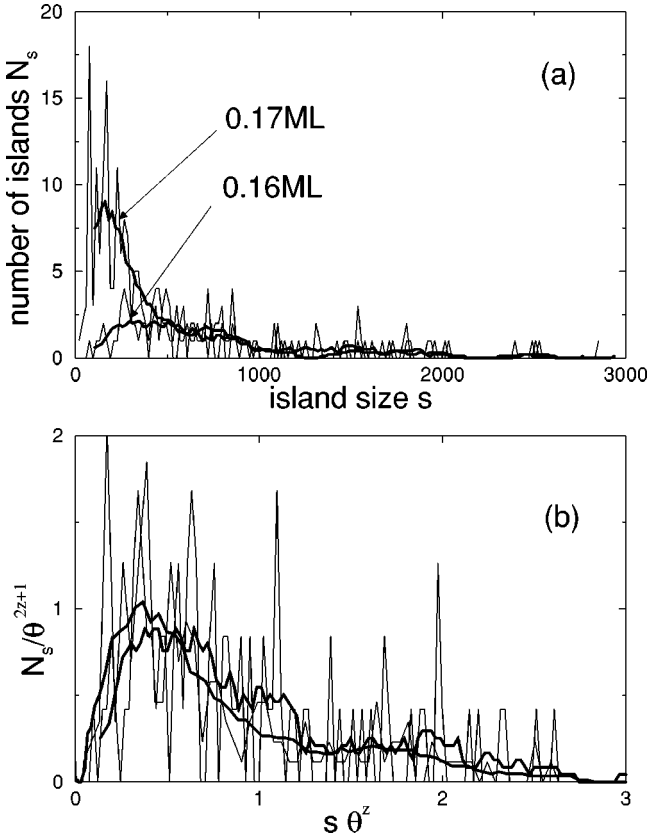

FIG. 9. Unscaled (a) and scaled (b) experimental island size distributions. Thin lines are original data. The thick lines are averages over 10 points. The corresponding exponents z are 2.30 and 2.38 at coverages 0.17 and 0.16 ML, respectively. The coverage used here is calculated based on the area covered by Ge islands. We note that this is different from the coverage calculated from the product of deposition flux and deposition time, which was used as the coverage in experimental measurements (Refs. 16–18).

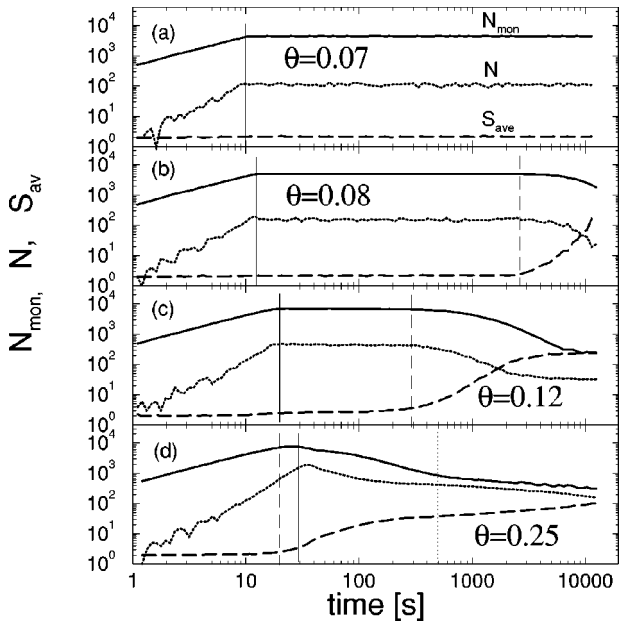

FIG. 10. Time evolution of number of monomers N_{mon} (solid lines), total number of clusters N (dotted lines), and average cluster size s_{av} (dashed lines). Solid, dashed, and dotted vertical lines indicate the end of evaporation time, formation of critical clusters, and the beginning of the Ostwald ripening, respectively. Deposition flux is 0.2 BL/min in all diagrams.

interesting to know how the systems would evolve if exchange with the surfactant were forbidden. This can be realized by setting the activation energy high enough to make exchange less probable. In this case the clustering above surfactant will develop without a time limit because the cluster growth is assumed to be reversible.

The idea of a critical cluster has been introduced to describe clustering.[50] A cluster has a critical size if it is in equilibrium with the surrounding monomers. The size of the critical cluster depends on the monomer concentration. An increase in monomer concentration results in a decrease of the critical cluster size and vice versa. Clusters larger than critical size tend to grow while smaller ones tend to dissociate. The last stages of the cluster formation have been described by Lifshitz and Slyozov.[50] The theory, also known as Ostwald ripening, has been developed for three-dimensional clustering, but has been modified and used to describe also the two-dimensional growth.[51–57] The theory assumes that clusters can grow and dissociate but cannot diffuse. A powerlike dependence of a critical cluster size with time is predicted.

During the simulation run the number of monomers N_{mon}, the total number of clusters N, and the average cluster size s_{av} are registered at different final coverages (Fig. 10). The coverage of $\theta=0.07$ is lower than a threshold one. After deposition (solid vertical line) the values of N_{mon}, N, and s_{av} remain almost unchanged.

The coverage $\theta=0.08$ [Fig. 10(b)] is a little above the threshold, and clusters start to grow after about 3000 s (dashed line). A time period between 10 s and 3000 s is needed to form clusters larger than critical. (Note that there is a repulsive interaction between monomers.) At the coverage $\theta=0.12$ the development of the cluster morphology is similar, but the time needed to create critical clusters is shorter.

At the coverage $\theta=0.25$, which is much larger than the threshold value, the critical clusters are formed before the deposition is completed. (Note the position of the dashed line in respect to the solid one.) The coverage is already high, and this results in a large number of clusters with an average size of $s_{av}\sim 3$. The growth occurs due to incoming monomers as well as due to subsequent cluster diffusion. After about 700 s (marked as a dotted vertical line) the monomer concentration is considerably lower, and the corresponding critical cluster size is larger. The time dependence of s_{av} begins to be powerlike (a straight line in a log-log plot with an exponent of about 0.28). Large clusters grow due to dissociation of smaller ones. Within this time interval the Ostwald ripening mechanism predominates.

Changes in cluster morphology with time differ much depending on the final coverage. The following stages can be distinguished: deposition, aggregation, and coalescence due to cluster diffusion and due to Ostwald ripening. Below the threshold only the deposition and aggregation regimes are

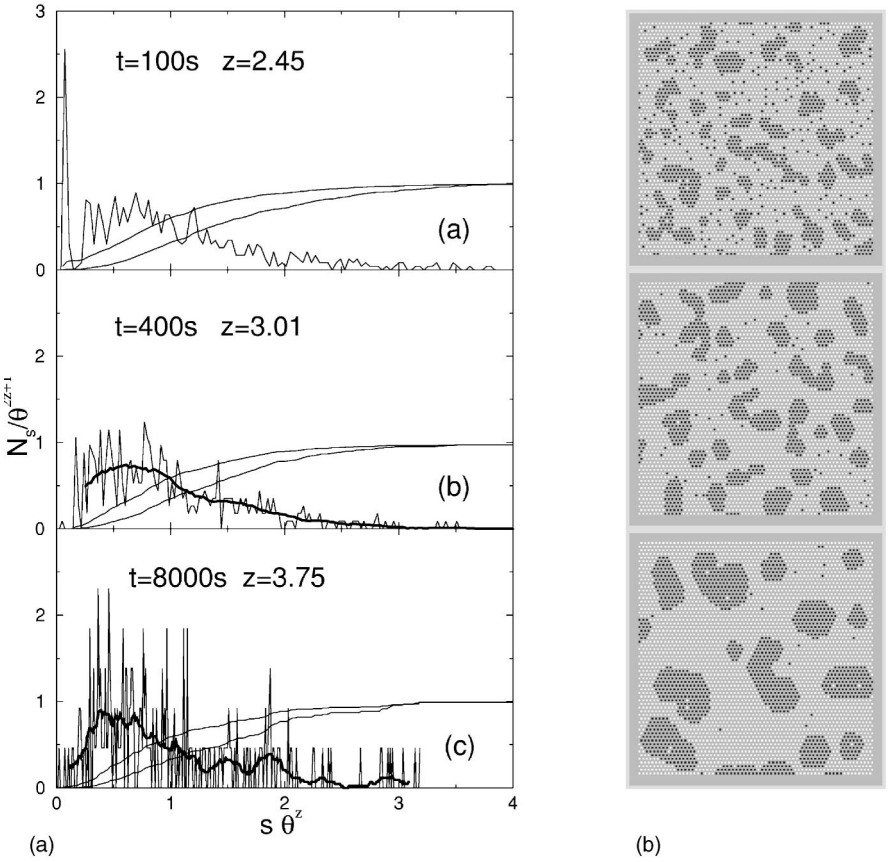

FIG. 11. The time evolution of the scaled island size distribution in the case when the exchange with surfactant is forbidden. The solid thin lines are the simulation results. The thick lines are averages over 20 points. Coverage $\theta = 0.3$. On the right-hand side we show the corresponding island morphologies.

seen within three hours of the simulation run. Above the threshold the aggregation time is shorter, followed by cluster diffusion. At coverages much higher than the threshold value the aggregation regime occurs within the deposition time, and is followed by cluster diffusion and a pronounced Ostwald ripening.

A. Self-similarity in cluster size distribution

At coverages well above the threshold the coalescence of clusters begins immediately after deposition [Fig. 10(d)]. In this case a sufficient number of clusters have been formed already during the deposition time, and the cluster size distributions may then be calculated.

The self-similar shapes of scaled cluster size distributions are obtained after applying the anomalous scaling procedure (Fig. 11). The scaling functions have maxima at normalized sizes smaller than 1. The exponent z is a time-dependent scaling factor. Its time dependence is presented in Fig. 12. Inflection points on the diagram correspond to a crossover between coarsening due to cluster diffusion and due to Ostwald ripening.

The above result agrees with the theory by Lifshitz and Slyozov[50] which predicts self-similarity. Discrepancy appears, however, on comparison of the shapes of the scaling functions, since the results obtained by Kandel[26] (maximum of scaling function at about 0.5) and by Lifshitz and Slyozov[50] (maximum of scaling function at about 1.0) significantly differ from each other. Our simulations show that the shape of the scaling function formed during the early stage of coarsening is conserved after the crossover from coalescence due to island diffusion to coalescence due to Ostwald ripening.

V. CONCLUSIONS

The formation of an island in a model for the Pb-mediated growth of Ge on Si(111) consists of the following steps: (i) a reversible formation of a Ge cluster above surfactant, (ii) an irreversible exchange of the cluster with surfactant (which forms an island seed), and (iii) growth of the island below the surfactant. Those processes make the SME growth much

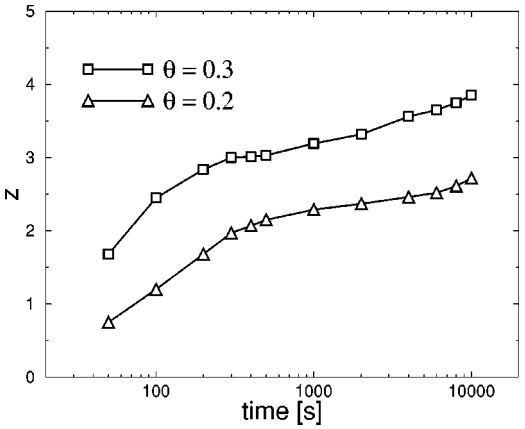

FIG. 12. Time dependence of the exponent z for cluster evolution in which exchange with the surfactant is forbidden.

more complex than growth without the assistance of the surfactant.

Interactions between Ge atoms are included during the clustering process. Their strength depends on the number of bonds with the nearest neighbors. A repulsive interaction is assumed in the case of one bond, and an attractive one, which gradually grows with the number of bonds, otherwise. Such interactions yield first the threshold coverage, and second the compact shape of Ge clusters. It was found that the clustering process obeys an anomalous scaling, and that the cluster size distribution is self-similar in time, up to the latest stages of coarsening where the Ostwald ripening mechanism predominates.

An irreversible collective exchange of Ge atoms with the surfactant forms an island seed; this process is then followed by subsequent growth of islands below the surfactant. After exchange the Ge atoms are not allowed to change position, and subsequent growth leads to island ramification. The above assumptions result in compact islands at high coverages and low temperatures; otherwise the islands assume a fractallike shape. It was found that the compact islands, obtained both experimentally and in Monte Carlo simulations, have the shape of the scaling function similar to those obtained within the cluster diffusion model of epitaxial growth.[26]

ACKNOWLEDGMENTS

This research is supported by the National Science Council of the Republic of China (Contract No. NSC89-2119-M-001-049) and Academia Sinica.

*Corresponding author. Electronic address: janusz@phys.sinica.edu.tw

[1] M. Copel, M. C. Reuter, E. Kaxiras, and R. M. Tromp, Phys. Rev. Lett. **63**, 632 (1989).
[2] W. F. Egelhoff, Jr. and D. A. Steigerwald, J. Vac. Sci. Technol. A **7**, 2167 (1989).
[3] S. Esch, M. Hohage, T. Michely, and G. Comsa, Phys. Rev. Lett. **72**, 518 (1994).
[4] J. Hrbek, A. K. Schmidt, M. C. Bartelt, and R. Q. Hwang, Surf. Sci. **385**, L1002 (1997).
[5] R. M. Tromp and M. C. Reuter, Phys. Rev. Lett. **68**, 954 (1992).
[6] H. Minoda, Y. Tanishiro, N. Yamamoto, and K. Yyagi, Surf. Sci. **357-358**, 418 (1996).
[7] M. Katayama, T. Nakayama, M. Aono, and C. F. McConville, Phys. Rev. B **54**, 8600 (1996).
[8] S. Dreiner, C. Westphal, F. Sökeland, and H. Zacharias, Appl. Surf. Sci. **123**, 610 (1998).
[9] M. Horn-von Hoegen, F. J. M. Heringdorf, M. Kammler, C. Schaeffer, D. Reinking, and K. R. Hofmann, Thin Solid Films **343-344**, 597 (1999).
[10] T. Fujino, T. Fuse, J. Ryu, K. Inudzuka, T. Nakano, K. Goto, Y. Yamazaki, M. Katayama, and K. Oura, Thin Solid Films **369**, 25 (2000).
[11] R. M. Tromp, IBM J. Res. Dev. **44**, 503 (2000).
[12] T. Lewowski and P. Wieczorek, Appl. Surf. Sci. **93**, 85 (1996).
[13] T. Lewowski, H. Otop, and P. Wieczorek, Appl. Surf. Sci. **103**, 35 (1996).
[14] B. Voigtländer, A. Zinner, T. Weber, and H. P. Bonzel, Phys. Rev. B **51**, 7583 (1995).
[15] H. Hibino, N. Shimizu, K. Sumitomo, Y. Shinoda, T. Nishioka, and T. Okano, J. Vac. Sci. Technol. A **12**, 23 (1994).
[16] I.-S. Hwang, T.-C. Chang, and T. T. Tsong, Phys. Rev. Lett. **80**, 4229 (1998).
[17] T.-C. Chang, I.-S. Hwang, and T. T. Tsong, Phys. Rev. Lett. **83**, 1191 (1999).
[18] I.-S. Hwang, T. C. Chang, and T. T. Tsong, Jpn. J. Appl. Phys., Part 1 **39**, 4100 (2000).
[19] J. Massies and N. Grandjean, Phys. Rev. B **48**, 8502 (1993).
[20] Z. Zhang and M. G. Lagally, Phys. Rev. Lett. **72**, 693 (1994).
[21] I. Markov, Phys. Rev. B **50**, 11 271 (1994).
[22] T. Ohno, Phys. Rev. Lett. **73**, 460 (1994).
[23] B. D. Yu and A. Oshiyama, Phys. Rev. Lett. **72**, 3190 (1994).
[24] A. Zangwill and E. Kaxiras, Surf. Sci. **326**, L483 (1995).
[25] D. Kandel and E. Kaxiras, Phys. Rev. Lett. **75**, 2742 (1995).
[26] D. Kandel, Phys. Rev. Lett. **79**, 4238 (1997).
[27] I. Markov, Surf. Sci. **429**, 102 (1999).
[28] B.-G. Liu, J. Wu, E. G. Wang, and Z. Zhang, Phys. Rev. Lett. **83**, 1195 (1999).
[29] J. Wu, B.-G. Liu, Z. Zhang, and E. G. Wang, Phys. Rev. B **61**, 13212 (2000).
[30] J. Bęben, I.-S. Hwang, T.-C. Chang, and T. T. Tsong, Phys. Rev. B **63**, 033304 (2001).
[31] K. A. Fichthorn and W. H. Weinberg, J. Chem. Phys. **96**, 1090 (1991).
[32] K. Binder and D. W. Heermann, *Monte Carlo Simulation in Statistical Physics* (Springer-Verlag, Berlin, 1992).
[33] T. T. Tsong and R. Casanova, Phys. Rev. B **24**, 3063 (1981); Phys. Rev. Lett. **47**, 113 (1981).
[34] J. A. Venables, G. D. T. Spiller, and M. Hanbücken, Rep. Prog. Phys. **47**, 399 (1984).
[35] H. Brune, Surf. Sci. Rep. **31**, 121 (1998).
[36] M. C. Bartelt and J. W. Evans, Phys. Rev. B **46**, 12 675 (1992).
[37] J. G. Amar, F. Family, and P.-M. Lam, Phys. Rev. B **50**, 8781 (1994).
[38] H. J. Ernst, F. Fabre, and J. Lapujoulade, Phys. Rev. B **46**, 1929 (1992).
[39] E. Kapatzki, S. Gunther, W. Nichtl-Pechar, and R. J. Behm, Surf. Sci. **284**, 154 (1993).
[40] J. A. Stroscio and D. T. Pierce, Phys. Rev. B **49**, 8522 (1994).
[41] Y. W. Mo, J. Kleiner, M. B. Webb, and M. G. Lagally, Phys. Rev. Lett. **66**, 1998 (1991).
[42] B. Muller, L. Nedelmann, B. Fischer, H. Brune, and K. Kern, Phys. Rev. B **54**, 17 858 (1996).
[43] J. Li, A. G. Rojo, and L. M. Sander, Phys. Rev. Lett. **78**, 1747 (1997).
[44] M. Smoluchowski, Phys. Z. **17**, 585 (1916).
[45] P. Meakin, Physica A **165**, 1 (1990).
[46] A. Lo and R. T. Skodje, J. Chem. Phys. **112**, 1966 (2000).
[47] C. R. Stoldt, C. L. Jenks, P. A. Thiel, A. M. Cadilhe, and J. W. Evans, J. Chem. Phys. **111**, 5157 (1999).
[48] I. Doudevski and D. K. Schwartz, Phys. Rev. B **60**, 14 (1999).

[49] P.-M. Lam, D. Bayayoko, and X.-Y. Hu, Surf. Sci. **429**, 161 (1999).
[50] I. M. Lifshitz and V. V. Slyozov, J. Phys. Chem. Solids **19**, 35 (1961).
[51] R. Barel, Y. Mai, G. R. Carlow, and M. Zinke-Allmang, Appl. Surf. Sci. **104/105**, 669 (1996).
[52] G. R. Carlow and M. Zinke-Allmang, Phys. Rev. Lett. **78**, 4601 (1997).
[53] G. R. Carlow, R. J. Barel, and M. Zinke-Allmang, Phys. Rev. B **56**, 12 519 (1997).
[54] H. Xia and M. Zinke-Allmang, Physica A **261**, 176 (1998).
[55] M. Iwamatsu, J. Appl. Phys. **86**, 5541 (1999).
[56] A. Raab and G. Springholz, Appl. Phys. Lett. **77**, 2991 (2000).
[57] V. P. Zhdanov, Eur. Phys. J. B **19**, 97 (2001).